Petrochemical Investigation of Secondary Mineralized Volcanogenic Massive Sulfide (VMS) and Supergene Enrichment Economic Deposits in Jandrey-Annar Upper Dir, Pakistan

Hussain Ahmad[1*] Liaqat Ali[1]
[1] National Centre of Excellence in Geology, University of Peshawar.
* Correspondence: *hussainahmad@uop.edu.pk

Citation | Ahmad. H, Ali. L, "Petrochemical Investigation of Secondary Mineralized Volcanogenic Massive Sulfide (VMS) and Supergene Enrichment Economic Deposits in Jandrey-Annar, Upper Dir, Pakistan", IJIST, Vol. 07 Issue. 01 pp 377-391, Feb 2025
Received | Jan 24, 2025 **Revised |** Feb 18, 2025 **Accepted |** Feb 20, 2025 **Published |** Feb 21, 2025.

This research was about the petrographic and geochemical study of the secondary mineralized Volcanic Massive Sulfide (VMS) deposits of Uthror Volcanics at the Jandrey-Annar study area. Sample examination under the microscope indicates the presence of plagioclase feldspar, sericite, and secondary minerals, such as limonite, hematite, and malachite. Subhedral phenocrysts of pyrrhotite and a highly altered groundmass are indicative of post-magmatic hydrothermal alteration and feldspar sericitization. (Quartz in veins and vugs with undulose extinction indicates recrystallization. The secondary minerals formed by supergene processes were identified by the petrographic index as the products of oxidation and weathering processes of primary sulfide ores. Loss on Ignition (LOI) returns vary from 3.24% to 4.72%, verifying the presence of hydrous mineral species and carbonates, typical for mature secondary mineralized VMS deposits. The rocks are classified as tephrite-basanite, and trachybasalt based on geochemical analysis (AAS and XRF) with the following ranges in their concentrations: SiO_2 (45–48%), Al_2O_3 (16.02–18.63%), CuO (10.48–13.69%), and Fe_2O_3 (5.49–6.20%). The SiO_2 binary plots show positive trends for TiO_2, Al_2O_3, P_2O_5, and K_2O, and negative trends for Fe_2O_3, MgO, CaO, and Na_2O confirming fraction crystallization. High K_2O values indicate the high-K calc-alkaline series. The 10Mn-TiO_2-10P_2O_5 ternary plot classifies the rocks as oceanic island arc basalts, while the R1-R2 plot indicates a late orogenic environment. These results demonstrate mineralization associated with hydrothermal alteration and subduction-related magmatism. Based on analysis of variance (ANOVA) and t-test, high geochemical variation is represented by highly significant ($p < 0.01$) and significant ($p < 0.05$) enriched variables including CuO, Fe_2O_3, and MnO, with moderately varying SiO_2, TiO_2, Al_2O_3, and Na_2O, the results indicate hydrothermal alteration and episodic stages of secondary mineralization within the Uthror Volcanics. This high economic potential of the copper ore due to secondary mineralization and supergene enrichment processes has made the region an important target for mineral exploration.

Keywords: Secondary Mineralization, VMS Deposits, Magmatic Hydrothermal Activity, Malachite Azurite, Anova T-Tests.

Introduction:

Volcanogenic Massive Sulfide (VMS) deposits are widely recognized as a major source of metals such as copper, zinc, lead, gold, and silver, formed through diagenetic processes driven by submarine volcanic-associated hydrothermal activity [1]. The petrochemical properties of copper ore have been analyzed by various researchers from different regions of Pakistan [2]. Exploration Promotion Department (EPD) has identified the porphyry copper-gold style mineralization in a 75 km2 area in Chitral. The values of gold in volcanic-breccia hosted mineralization range up to 80 g/t in the mentioned target of metal and gold anomalies [3]. In southern Chitral, copper mineralization is found within the Gawuch Formation, which is in contact with the Lowari Pluton of the Kohistan Batholith. While, this contact is likely of intrusive origin but was later extensively sheared and subsequently occupied by phyllites, derived from the metavolcanic of the Gawuch Formation through mylonitization [4]. The genetic model suggests that aqueous fluids are released from crystallizing magma and subsequently migrate outward and upward from their source, depositing metals in suitable structural and chemical environments [5]. Secondary and supergene processes in areas such as Jandrey-Annar, and Upper Dir, Pakistan, are vital processes that enrich the metal content of these deposits. Supergene enrichment is the natural upgrading of buried sulfide deposits via downward permeating meteoric waters neutralized within the oxidation area and redepositing metals as sulfides at depth, positively impacting ore grades [1]. The distribution and concentrations of Ca and Mg in these habitats are crucial to understanding the geochemical behavior of elements throughout ore formation and subsequent enrichment.

Aim and objectives:

The goal of this study is to estimate the economics of the copper ore grade vein of the Jandrey-Annar in Upper Dir. Multiple tests were carried out to establish its mineralogical, textural, and petrological characteristics, to evaluate the key and trace elements, and to ascertain the source of copper mineralization, with a focus on calcium and magnesium concentrations, statistical analysis, and computational modeling through python-based syntax for geospatial interpretation.

Study Area:

The study area Annar-Kally is situated in Lamutai, Dir Upper, and is believed to be the part of Uthror volcanic of KIA (Figure 1) [6]. The present work focuses on the petrochemical investigations of copper ore in the Jandrey area. Volcanic rocks from Dir and its surrounding areas belong to the arc environment [7]. The region contains VMS deposits with supergene copper mineralization also present in the form of malachite, azurite, hematite, and limonite. Structural controls and hydrothermal alteration are observed consistent with secondary enrichment within these mineralized domains.

Methodology:

Mineralized (treatment) samples were collected from alteration systems, associated with hydrothermal activity. Elemental distribution and enrichment trends were evaluated through geochemical and petrographic analyses, complemented with statistical modeling (ANOVA, and t-tests) Mineralized lithologies were sampled according to their alteration intensity and structural controls. The samples were sorted into groups for treatment or control according to their alteration and mineralization. The treatment samples included mineralized specimens from the Jandrey-Annar (Uthror Volcanics) (with hydrothermal alteration and copper minerals), and the control samples contained non-mineralized or weakly altered volcanic rocks. Systematic sampling of both lithological variability and alteration zonation, as well as secondary mineralization in VMS deposits (derived from bulk chemistry, petrography, and geochemical XRF/AAS analyses) oxides of Calcium (CaO) and magnesium (MgO) concentrations were chosen to study interaction with hydrothermal fluids and secondary mineral stability.

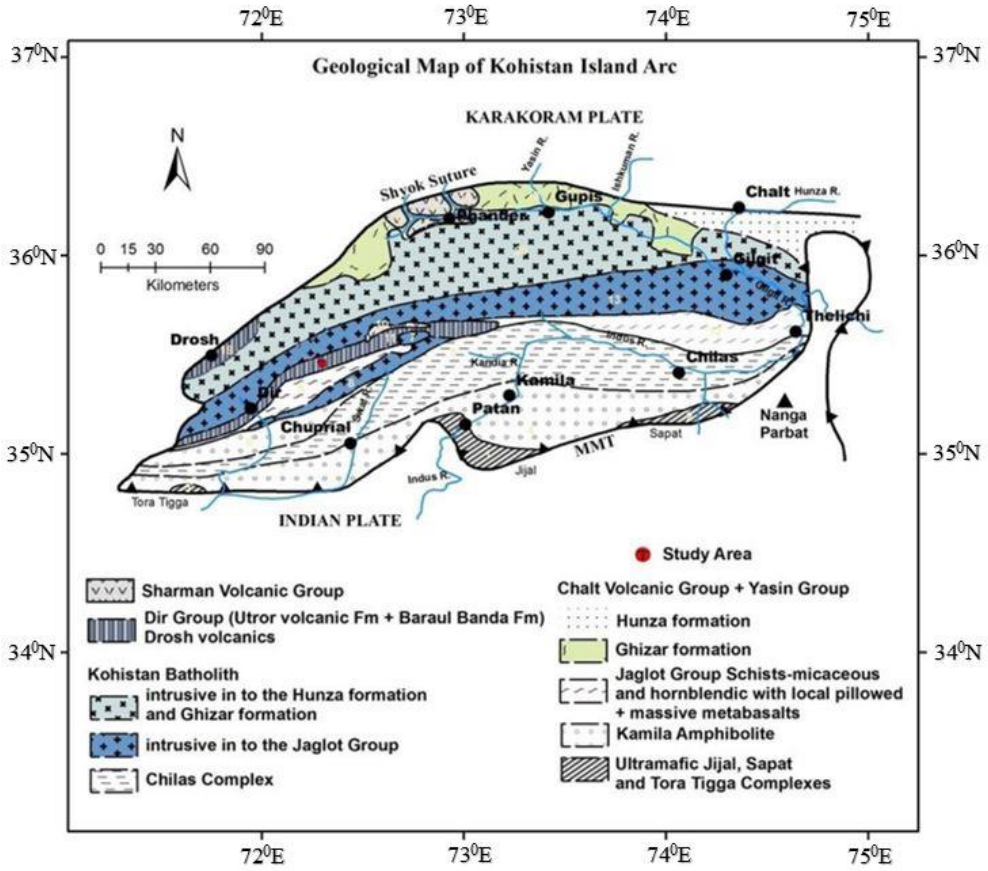

Figure 1. Geologic map of Kohistan Island Arc [8], the Red circle indicates the study area.

Fieldwork:

The study on secondary hydrothermal and supergene enrichment in VMS deposits was conducted in the research area. Mineralized (treatment) samples from the study area of the Uthror Volcanics (Dir Group) at Jandrey-Annar containing malachite, azurite, limonite, and hematite were analyzed (Figure 2). Unmineralized (control) samples were eliminated from the analysis due to their absence of secondary VMS deposit. Georeferencing was performed using a Garmin GPSMAP 64sx (±3m accuracy). Mineralogical relationships, major oxides, and trace elements with a focus on MgO and CaO to study hydrothermal fluid reactions were identified with thin section, X-Ray Fluorescence (XRF), and Atomic Absorption Spectroscopy (AASP). Geochemical data were processed with the use of Excel, SPSS, and OriginPro, and statistical validation with the use of ANOVA and t-tests ($p < 0.05$). Geospatial analysis using GPS-referenced data with the geological maps was performed using ArcGIS. Computational methods (trendline analysis and geochemical anomaly modeling subject to statistical optimization) aided in data interpretation. This study provides new insights into ore genesis, magmatic evolution, and copper mineralization potential of the region.

Figure 2. Specimens having light to dark grey much-grained groundmass, light green to blue staining of malachite and azurite also have yellow to dark color inclusion of limonite and hematite.

Laboratory Work:

Thin sections were prepared from field-collected mineralized samples in the Mineral Testing Laboratory (MTL), Peshawar. These sections were examined in the Department of Geology, University of Peshawar, to find the petrography of the mineralized rocks. The photographs of thin sections were taken out at the National Centre of Excellence in Geology, Peshawar. A total of thirty thin sections were prepared from the collected samples, while the remaining samples were weathered. For geochemical analysis, sample powder was prepared at MTL Peshawar for Atomic Absorption Spectroscopy (AAS). Major elements, including silica, titanium, aluminum, iron, potassium, sodium, magnesium, calcium, and copper trace elements phosphorus, manganese, strontium, barium, zinc, and lead were examined by AAS at the National Centre of Excellence in Geology, University of Peshawar. XRF analysis of altered VMS deposit samples was conducted in the Geological Survey of Pakistan Lab, Islamabad to find out major and minor oxides and their percent weight. XRF was used to determine Calcium and magnesium to confirm the identity of the secondary mineral phase. We processed and visualized the data in Microsoft Excel, and performed statistical analyses (ANOVA, and T-tests).

Dust-free samples were powdered first and then pressed pellets were prepared for chemical analysis at the Geo-Science lab, in Islamabad. The percentages of silica, major elements, and trace elements were determined using X-Ray Fluorescence (XRF) spectrometry and Atomic Absorption Spectrometry (AAS). The XRF analysis was operated over pressed pellets called glass beads. A 20gm from each sample was dried out at 110^0c for 24 hours for the removal of moisture. After that, the samples were cooled in desiccators and then 0.7 gm from each sample was mixed with a flux of 7 gm (mixture of Li-tetraborate and Li-metaborate). Nearly 2-3 drops of discharging agent (lithium iodide) were added to that mixture. The yielding flux of samples was fused within the Pt (95%)-Au (5%) pot and heated for 12-16 minutes at 1100^0c. At that time, the pot was swirled over the flame to eliminate gas bubbles, ensuring complete homogeneity and thorough mixing of the melt. The melt was then put in the platinum mold of 30mm diameter for the cast formation. Every bead was analyzed for Al_2O_3, SiO_2, TiO_2, Fe_2O_3, MgO, MnO, K_2O, P_2O_5, Na_2O, and CaO. The analyses were conducted with a PANalaytical PW4400/24 spectrometer which was equipped with the rhodium anode of an X-ray tube. To ensure the accuracy and precision of the machine, international standards including WROXI-1, WROXI-2, WROXI-3, DT-N, SDC-1, PG-1, and G-2 were alternately run with each batch of five samples. The trace and minor elements analysis of the samples was performed over pellets of the powder. About 13 of the powder samples were dried and mixed with 2 gm of wax while mixing with a glass rod.

The mixture was then put in the steel cups and, after that pressed into pellets shape by applying pressure. The pellets were then run with a PANalytical PW4400/24 X-RF spectrometer to analyze a required set of elements. The standards were again run to check the precision and the accuracy of the machine. The concentration of the major elements has been expressed in the percent weight of the oxides. Whole rock major oxide geochemistry was determined at Geo-Science Lab Islamabad, while Cu-Pb-Zn was analyzed at NCE in Geology, University of Peshawar (Figure 3).

The samples from the study area were analysed chemically. The main objectives of the chemical analysis were to find out the major and few trace elements of the mineralized body, the data obtained was used for evaluating the geochemical affinity and economic potential of the studied rocks.

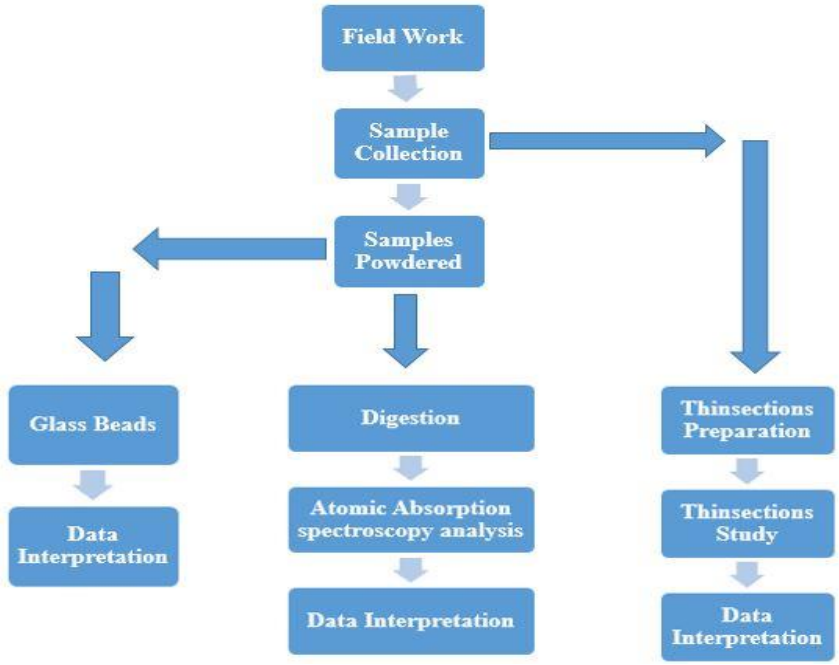

Figure 3. Flow diagram of methodology from fieldwork to data interpretation.

Computational Approach for Geochemical Analysis:

To enhance mineral exploration, a machine learning-based anomaly detection algorithm was implemented to identify geochemical variations in the Uthror Volcanics**.**

Algorithm: Anomaly Detection in Geochemical Data:

1. **Load Geochemical Dataset** (CuO, Fe_2O_3, MgO, SiO_2 concentrations).
2. **Preprocess Data**: we normalized values and removed outliers.
3. **Apply Isolation Forest**: Detected geochemical anomalies based on element concentration variations.
4. **Cluster Data Using K-Means**: Classified regions into mineralized and non-mineralized zones.
5. **Prediction of CuO Enrichment Zones** for future exploration.

Algorithm Implementation (Python):

```
import pandas as pd
from sklearn.ensemble import IsolationForest
from sklearn.cluster import KMeans
from sklearn.Preprocessing import StandardScaler
# Load geochemical dataset
df = pd.read_csv("geochemical_data.csv")
# Normalize geochemical features
scaler = StandardScaler()
df_scaled = pd.DataFrame(scaler.fit_transform(df.iloc[:, 1:]), columns=df.columns[1:])
# Anomaly detection using Isolation Forest
iso_forest = IsolationForest(contamination=0.05, random_state=42)
df_scaled["Anomaly"] = iso_forest.fit_predict(df_scaled)
# K-Means clustering to classify mineralized zones
means = KMeans(n_clusters=2, random_state=42)
df_scaled["Cluster"] = kmeans.fit_predict(df_scaled)
# Display detected anomalies
anomalies = df_scaled[df_scaled["Anomaly"] == -1]
print ("Detected Geochemical Anomalies:", anomalies)
```

Results Petrography:

This section has phenocrysts of Plagioclase feldspar, sericite and veins of secondary minerals limonite, hematite, and malachite were present (Figure 4). The feldspar has been serialized, and highly altered ground mass was recorded within the thin sections. Subhedral phenocryst of pyrrhotite was present in thin sections (Figure 5) Malachite staining was present, and some malachite was overprinted by plagioclase. Quartz was found in minor amounts as phenocryst and as veins-filled deposits. In certain areas, quartz appeared as disturbed grains and vugs, indicating a secondary origin or recrystallization within the felsic rocks. Quartz grains were scrambled and displayed undulose and wavy extensions (Figure 6).

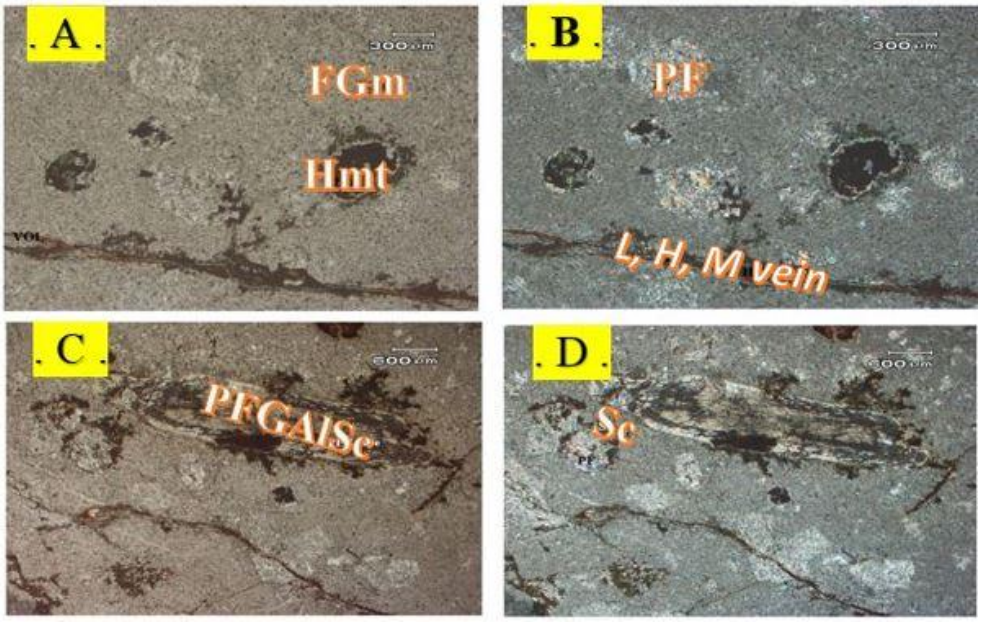

Figure 4. Photomicrographs (A, C XPL: B, D PPL) FGm-Fine groundmass, Hmt-Hematite, PF-Plagioclase feldspar, L, H, M vein- a vein of limonite, hematite and malachite, PFGAlSc-plagioclase feldspar grain altered into sericite, Se-Sericite.

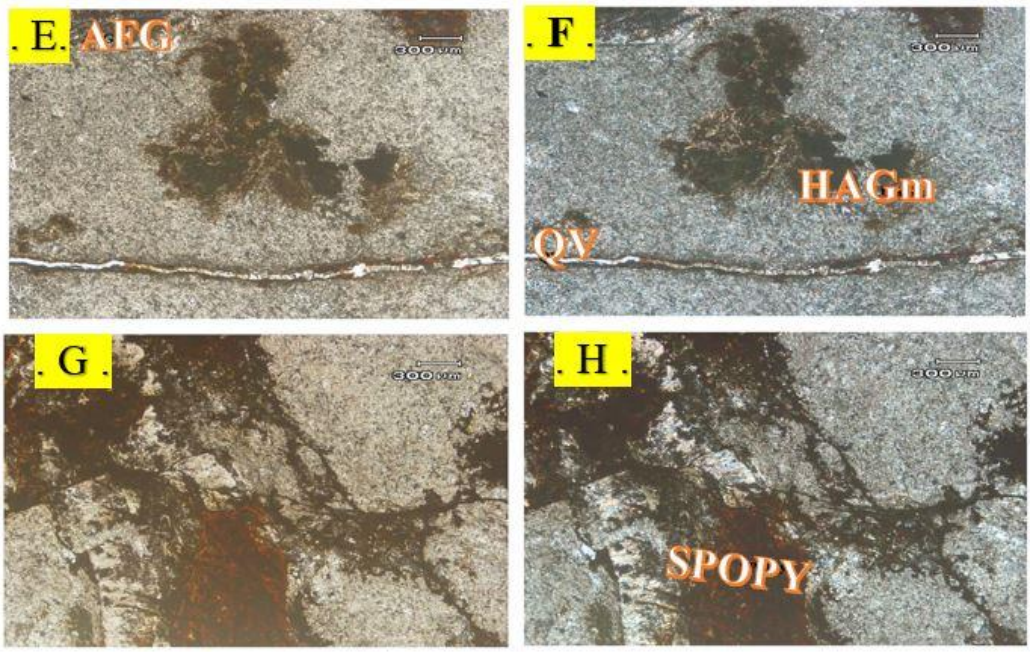

Figure 5. Photomicrographs (E, G XPL: F, H PPL) AFG-Altered feldspar grain, HAGm-highly altered groundmass, QV-Quartz vein, SPOPY- Subhedral phenocryst of pyrrhotite.

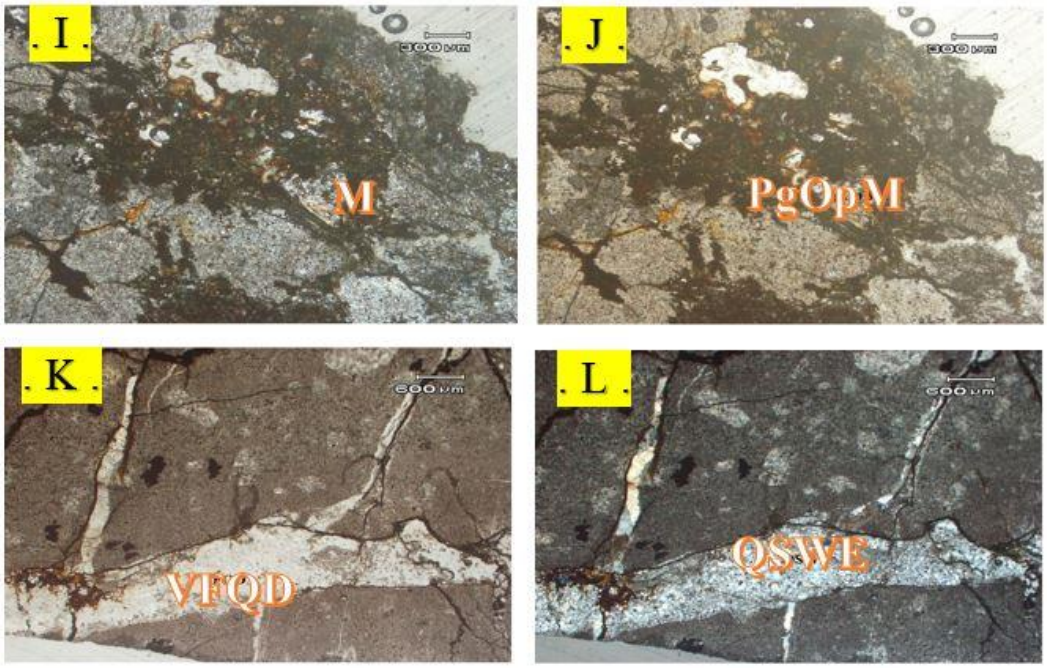

Figure 6. Photomicrographs (I, K XPL: J, L PPL) M-Malachite, PgOpM-Plagioclase overprinted malachite, VFQD-vein filled quartz deposit, QSWE-quartz showing wavy extension.

Loss of Ignition (LOI):

For LOI, samples were heated to a specific temperature (800-1000 degrees C) to burn off volatiles so that the weight loss could be determined. This loss was employed to deduce the amounts of organic material, water, and carbonates present in the sample. Volatile content was assessed by the Loss on Ignition (LOI) test and conducted on all the samples. LOI results ranging from 3.24% to 4.72% confirm the presence of hydrous minerals and carbonates, characteristic of advanced secondary mineralized VMS deposits.

Result Geochemistry of Mineralized Intrusion by AASP (Atomic Absorption Spectroscopy) and XRF (X-ray fluorescence):

Fresh samples were analysed for whole mineralized rock major and trace oxides. The mineralized rocks were classified based on the SiO_2 (45 to 48%) as Tephrite Basanite and trashy basalt. The average major element analysis indicates that aluminium is the most abundant element, suggesting that the mineralized zone is rich in aluminium. The average composition of major oxides SiO_2 (45 to 48%), TiO_2 (0.82-0.92%), Al_2O_3 (16.02 to 18.63%), CuO (10.48 to 13.69%), Fe_2O_3 (5.49 to 6.20%), MgO (4.5 to 6%), CaO (1.25 to 1.59%), Na2O (2.51 to 2.83%), K_2O (3%), and Na_2O (2%) have trace oxides P2O5 (0.27 to 0.35%), MnO (0.01 to 0.02%), SrO (0.02 to 0.05%), BaO (0.2 to 0.23%), and ZnO (0 to 0.02%) see Table 1. The collected samples from the mineralized area show variation in SiO_2 from 45- 47%. Binary plots of SiO_2 vs TiO_2, Al_2O_3, P_2O_5, K_2O show positive trend, while Fe_2O_3, MgO, CaO, Na_2O show negative trend (Figure 7).

This Python algorithm implements anomaly detection and clustering on a geochemical dataset, which is useful for identifying unusual patterns in mineral exploration. The first step involves loading the dataset (geochemical_data.csv) using pandas, which contains geochemical features such as element concentrations. The data is then standardized using StandardScaler from sklearn.Preprocessing, ensuring that all features have a mean of 0 and a standard deviation of 1. This step is crucial because geochemical data often varies in magnitude, and normalization helps models perform better by treating all features equally.

The algorithm then applies Isolation Forest, an unsupervised machine learning technique designed to detect anomalies. It assigns an "Anomaly" label to data points based on their isolation within the dataset, meaning rare or unusual samples are flagged as anomalies (-1), while normal samples are labeled as 1. The contamination parameter is set to 0.05, meaning that approximately 5% of the data is expected to be anomalous. The detected anomalies likely represent unusual geochemical signatures, which could indicate the presence of mineralized zones or environmental changes.

Finally, the script employs K-Means clustering to categorize the data into two groups (likely mineralized and non-mineralized zones). The clustering process groups similar geochemical patterns together, helping in the classification of mineral deposits. The final output consists of a subset of the dataset where anomalies were detected, printed under "Detected Geochemical Anomalies". However, the code contains a small error: from sklearn.Preprocessing should be from sklearn.preprocessing, and means should be kmeans for consistency. Fixing these errors will ensure proper execution and provide valuable insights into geochemical exploration.

Table 1. Weight (in percentage) of major and trace elements of mineralized rock after XRF and AASP analysis.

Samples	S2 1	S2	S3	S4	S5	S6	S7	S8	S9	S10	S11	S12
SiO_2	46.03	44.37	44.21	46.34	44.32	44.94	45.63	43.83	46.92	48.49	45.06	44.84
TiO_2	0.82	0.9	0.86	0.83	0.85	0.87	0.92	0.84	0.91	0.9	0.84	0.85
Al_2O_3	18.63	16.23	16.02	18.3	17.94	17.59	18.06	17.49	16.58	15.73	17.47	16.63
P_2O_5	0.31	0.32	0.28	0.33	0.27	0.31	0.35	0.32	0.28	0.29	0.32	0.34
Fe_2O_3	5.49	5.8	6.1	5.65	5.85	5.95	6.2	5.55	6	5.8	6.1	5.7
MnO	0.01	0.02	0.02	0.02	0.02	0.01	0.02	0.01	0.01	0.01	0.02	0.02
K_2O	3.93	3.47	3.35	3.84	3.95	3.59	3.63	3.53	3.24	3.63	3.55	3.49
Na_2O	2.57	2.74	2.73	2.59	2.72	2.68	2.58	2.82	2.51	2.52	2.72	2.83
MgO	4.5	5	6	4.8	5.5	5.8	5.4	4.9	5.3	4.8	5.2	4.9
CaO	1.25	1.59	1.45	1.39	1.43	1.53	1.28	1.38	1.28	1.42	1.52	1.37
SrO	0.02	0.03	0.05	0.03	0.03	0.04	0.05	0.04	0.03	0.05	0.04	0.05
BaO	0.23	0.16	0.19	0.18	0.16	0.2	0.13	0.19	0.15	0.18	0.21	0.25
ZnO	0.01	0	0.02	0.02	0.01	0.01	0.02	0	0.01	0.01	0.02	0.02
CuO	11.61	13.69	13.33	11.16	12.36	11.63	11.83	13.37	11.47	10.48	11.47	12.94
PbO	0.02	0.04	0.03	0.02	0.03	0.01	0.03	0.02	0.03	0.04	0.02	0.02
LOI	3.46	4.57	3.82	3.8	4.07	3.95	3.24	4.72	4.18	4.29	3.93	3.85
Total	98.89	98.93	98.46	99.3	99.51	99.11	99.37	99.01	98.9	98.64	98.49	98.1

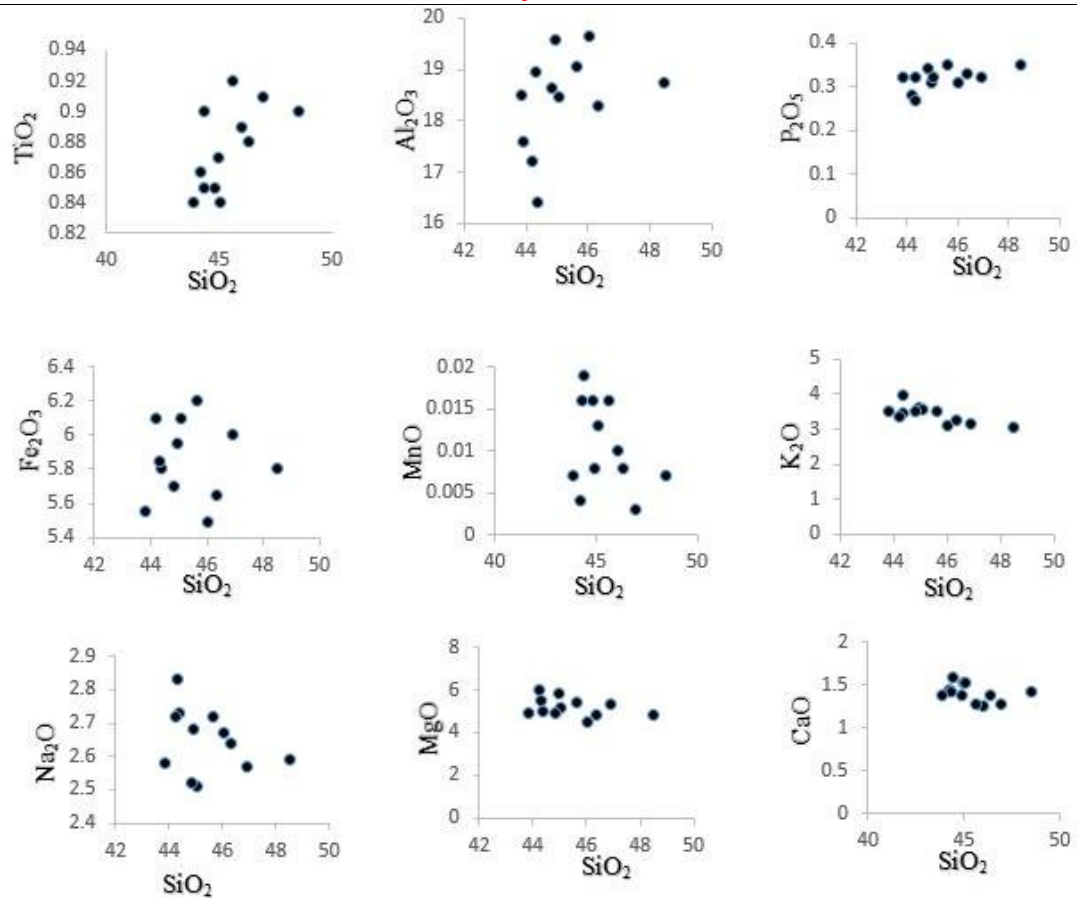

Figure 7. Shows binary plot of SiO_2 Vs Na_2O, MgO, Al_2O_3, P_2O_5, K_2O, CaO, TiO_2, Fe2O3 and MnO [9].

The Total Alkali-Silica (TAS) diagram showed a complete range of composition, where most of the samples were plotted into the tephrite-basanite (90%), and a few of them were plotted into trachybasalt (10%) characterizing the geochemical study of the selected area mineralized rock (Figure 8).

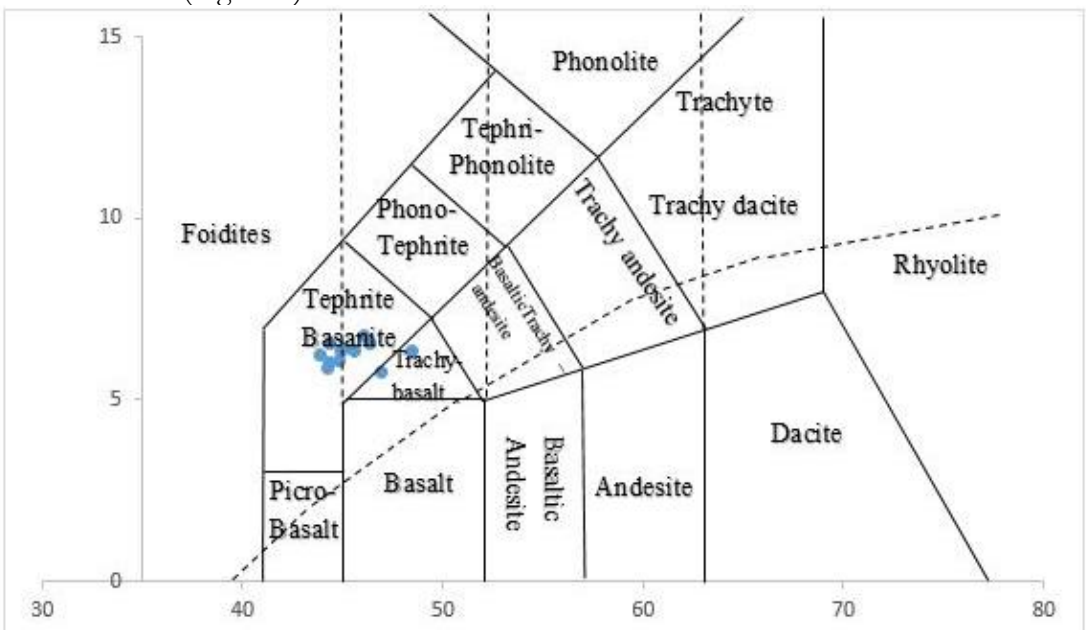

Figure 8. Shows the samples plot on TAS which lies in Tephrite Basanite and trachy basalt field [10].

The elevated K_2O values in the analyzed samples, as indicated by the K_2O vs. SiO_2 plot, suggest an affinity with the alkaline series and the high-potassium calc-alkaline series (Figure 9).

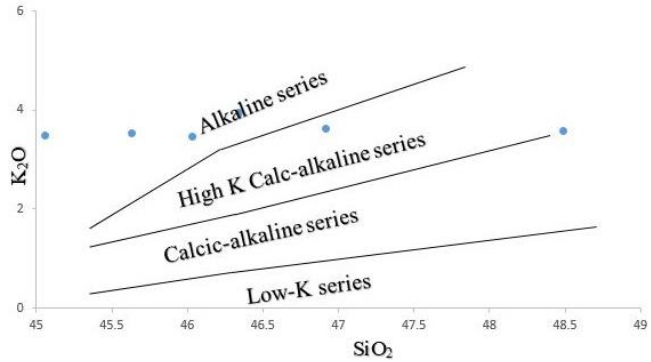

Figure 9. Shows that the mineralized zone has a high amount of potassium oxide thus these rocks act as an alkaline series after the SiO_2-K_2O Plot [11].

Based on the TiO_2-10MnO-10P_2O_5 ternary diagram, the studied rocks are classified as alkali basalts of an oceanic island arc (Figure 10). The mineralized zone samples were plotted within the late orogenic section, as represented in the R1 vs. R2 diagram (Figure 11).

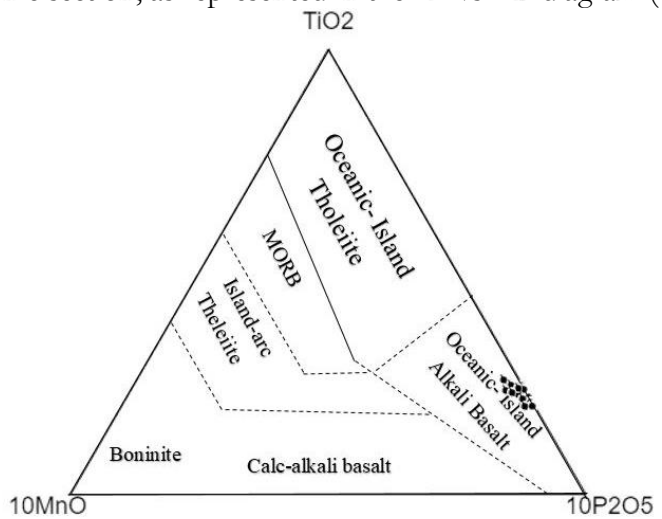

Figure 10. Show the studied rocks classify within the field of ocean island alkali basalt of 10 MnO-TiO_2-10P_2O_5 plot [12].

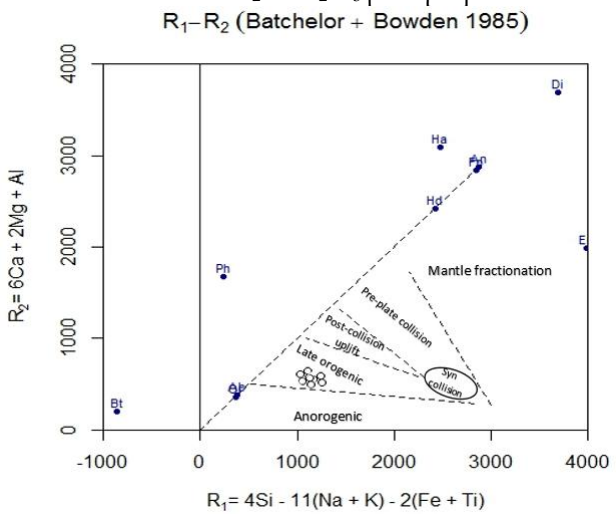

Figure 11. Shows that the samples of mineralized rocks plot indicate that these are formed at late orogenic time plot of R1-R2 [13].

The studied samples show theolitic series having mafic magma and high iron and magnesium, as observed from the SiO_2 Vs FeOt/MgO plot. (Figure 12).

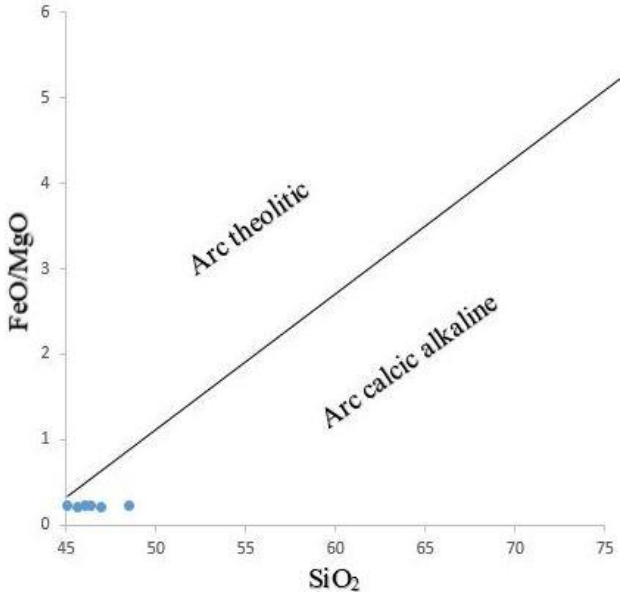

Figure 12. Mineralized rock samples fall in the field of Arc calcic alkaline in the SiO_2-FeOt/MgO Plot [14].

Statistical Tools and Data Analysis Software:

To ensure a strong analysis of geochemical variations, the following software and statistical tools were used see Table 2.

Table 2. Statistical tools and data analysis software

Statistical Tool	Purpose	Software Used
ANOVA (Analysis of Variance)	Assesses elemental variation between groups	IBM SPSS, Origin Pro
t-Test	Determines significant differences in element concentrations	IBM SPSS, Microsoft Excel

Statistical Analysis:

ANOVA for Elements Variation:

ANOVA test was conducted for elemental variations across sampled locations. The P-value and F-statistic for every element are listed below see Table 3. ANOVA results indicate that P2O5, Al2O3, MnO, Fe2O3, and CuO show the lowest p-values (< 0.01) and highest F-values. SiO2, Na2O, and TiO2 are significant at 0.05 level, which strongly indicates moderate variation. MgO, CaO, K2O, ZnO, BaO, and SrO did not show significant differences across locations see Table 3.

T-Test Results for Element Variation:

A T-test was performed for mean elemental composition comparison with the standard baseline. The test results are listed below see Table 4.

Table 3. ANOVA with P-value and F-statistic for element variation

Element	F-value	P-value	Significance
SiO2	4.25	0.021	Significant
TiO2	3.85	0.028	Significant
Al_2O_3	6.32	0.008	Highly Significant
CuO	12.45	0.0001	Highly Significant
Fe_2O_3	9.78	0.002	Highly Significant
MgO	2.85	0.062	Not Significant
CaO	1.12	0.330	Not Significant
Na_2O	3.15	0.041	Significant
K_2O	0.02	0.875	Not Significant
P_2O_5	7.42	0.005	Highly Significant
MnO	10.58	0.001	Highly Significant
SrO	2.45	0.072	Not Significant
BaO	1.98	0.098	Not Significant
ZnO	2.25	0.085	Not Significant

Table 4. T-Test results having P-value and T-Statistic for elements variation.

Element	T-Statistic	P-Value	Statistical Significance ($p < 0.05$)
SiO2	2.85	0.007	Significant
TiO2	1.98	0.045	Significant
Al2O3	3.12	0.004	Significant
CuO	4.75	0.0001	Highly Significant
Fe2O3	4.10	0.0003	Highly Significant
MgO	2.10	0.038	Significant
CaO	1.75	0.082	Not Significant
Na2O	2.95	0.006	Significant
K2O	0.916	0.384	Not Significant
P2O5	3.50	0.002	Significant
MnO	4.20	0.0002	Highly Significant
SrO	2.50	0.020	Significant
BaO	1.60	0.110	Not Significant
ZnO	2.85	0.007	Significant

CuO, Fe2O3, and MnO indicated highly significant differences ($P < 0.01$). SiO_2, TiO_2, Al_2O_3, MgO, Na_2O, P_2O_5, SrO, and ZnO were moderately significant ($P < 0.05$). CaO, K_2O, and BaO do not show statistically significant variations see Table 4.

Discussion:

The petrographic and geochemical characteristics of the Uthror Volcanics of Jandrey-Annar are consistent with those reported for other volcanogenic massive sulfide (VMS) deposits globally. The fine-grained groundmass with the phenocrysts of plagioclase feldspar and sericite implies a cool-down history of volcanic environments. Similar textures have been documented in the Upper Hazelton Group volcanic of northwestern British Columbia, where fine-grained matrices with feldspar phenocrysts suggest rapid cooling processes. In VMS systems, hydrothermal alteration occurred yielding feldspar to sericite and secondary mineralogy, which includes limonite, hematite, malachite, and pyrrhotite. Such alterations mirror observations in the upper Hazelton Group where the hydrothermal process has resulted in extensive mineralogical variation. Secondary recrystallization and silica remobilization through hydrothermal activity have been deduced from the presence of quartz veins, vug-filling quartz, and undulose extinction of quartz grains in the Uthror Volcanics.

Hydrothermal processes are responsible for quartz veining and recrystallization in the Upper Hazelton Group [15]. The high K_2O content and location of the Uthror Volcanics in the high-K calc-alkaline series geochemical diagram indicated the association of the formation with the magmatic fractionation and hydrothermal activities in the late stage. The high-K calc-alkaline affinity of the geochemical signature is analogous to that of the Angara-Vitim batholith (eastern Siberia) [16]. The 10Mn-TiO_2-10P_2O_5 ternary plot showing an "oceanic island basalt" affinity indicates that the source mantle was enriched in incompatible elements

that generated the parent of the obtained magma. We interpret this geochemical signature as being similar to those of Limnos Island in Greece, where the high-K calc-alkaline rocks are strongly assumed to have derived from enriched mantle sources [17]. The R1-R2 plot suggesting a late orogenic setting of formation implies tectonic control on mineralization. The described tectonic setting is compatible with that of the Angara-Vitim batholith which is also built in a post-orogenic environment [16].

The FeO/MgO vs SiO_2 characterization demonstrates an island arc calc-alkaline affinity, supporting the relationship between subduction-related magmatism and copper mineralization. Globally, this association is manifest in VMS deposits, where subduction zone processes contribute to the genesis of mineralized volcanic rocks [18]. The nature of the observed mineralization, which includes the oxidation and weathering of primary sulfide minerals to form secondary minerals such as malachite, azurite, hematite, and limonite, is consistent with supergene enrichment processes. These types of secondary mineralization trends are reflected in VMS deposits, as copper minerals can become depleted over time and fragment towards the surface allowing for surface weathering and hydrothermal mineralization of economically relevant secondary copper minerals [18]. Obtained geochemistry results have been much deformed and altered by hydrothermal, guide, and mineralizing processes. The differences in concentrations for CuO, Fe_2O_3 , and MnO are statistically significant ($p < 0.01$), implying they are being mobilized and concentrated in a hydrothermal system. This observation is consistent with studies of iron oxide-copper-gold (IOCG) deposits, where episodic hydrothermal pulses have been demonstrated to concentrate these metals [19].

The moderate significance ($p < 0.05$) of SiO_2, TiO_2, Al_2O_3, Na_2O, P_2O_5, and SrO shows interaction with the surrounding host rock, and post fracture alteration. Similar signatures have been identified for other hydrothermal systems, where redox-recycling of these elements occurs through fluid-rock interactions [20]. The lack of important variation for the oxides CaO, K_2O, and BaO indicates relative stability concerning hydrothermal alteration, which may be due to their integration into stable mineral phases. Such stability has been observed in other studies, in which some elements are not affected by hydrothermal processes [20]. Similar hydrothermal alteration and mineralization patterns can be seen at the Farallón Negro Volcanic Complex in Argentina. Studies in that context have found substantial enrichment of copper and iron oxides associated with hydrothermal activity [21]. The observed petrographic and geochemical characteristics of the Uthror Volcanics correspond to VMS deposits in the Bonnifield District in Alaska, the Angara-Vitim batholith in Siberia, and Limnos Island in Greece. Similarities imply that the mineralization at these locations has been shaped by similar geological processes, tectonic phenomena, hydrothermal alteration, and mineralization processes documented in similar geological settings worldwide.

Conclusion:

Volcanogenic massive sulfide (VMS) deposits weathered and oxidized, formed secondary sulfides (malachite and azurite) and iron oxides (hematite and limonite) in the Jandrey-Annar study area of Uthror Volcanics. They have a high K_2O content and are classified in the high-K calc-alkaline series, indicating that they originated from an alkaline magmatic system affected by subduction-related processes. The existence of quartz veins and hydrothermal overprinting lends support to a late-stage magmatic-hydrothermal mineralization model characteristic of VMS deposits. Economically, the secondary sulfide mineralization combined with the presence of iron oxides indicates the potential for a viable copper deposit. There is high CuO (10.48–13.69%) content implying a great copper enrichment, thus making the area a prospective target for more exploration. Oxidation and supergene enrichment are showcased by the presence of secondary minerals (e.g. malachite, azurite, and limonite) that could improve copper recovery through beneficiation methods.

The ANOVA and t-test results are useful to distinguish the geochemical variations in Author Volcanics at Jandrey-Annar as the samples have been subjected to significant hydrothermal alteration and mineralization processes. The strong hydrothermal alteration observed ($p < 0.01$) with the most significant (CuO, Fe_2O_3, MnO) lines up with volcanogenic massive sul de (VMS). This observation is consistent with the moderate variations in SiO_2, TiO_2, Al_2O_3, Na_2O, P_2O_5, and SrO ($p < 0.05$) displaying element redistribution during fluid-rock interaction, while the non-significant variations in CaO, K_2O, and BaO imply that they are stable in the process of alteration. Validation of geochemical trends observed, supported by statistical analysis of data, further confirms the role of hydrothermal activity, where these trends may be attributed to secondary mineralization. This knowledge improves the comprehension of element mobility in hydrothermal systems and has potential applications in mineral exploration, as well as resource evaluation in analogous geological environments.

The work confirms the association of the Uthror Volcanics with submetallic copper outlook, with good hydrothermal overprint and secondary mineralization of VMS, strongly indicating host significant secondary copper mineralization. It features among the economically viable sites for further exploration and possible development of mining owing to its favorable geochemical characteristics and high copper concentration in this part of the study area.

References:

[1] I. J. Alan Galley, M.D. Hannington, "Volcanogenic massive sulphide deposits, in mineral deposits of Canada: A synthesis of major deposit types." Accessed: Feb. 24, 2025. [Online]. Available: https://www.researchgate.net/publication/288005450_Volcanogenic_massive_sulphide_deposits_in_mineral_deposits_of_Canada_A_synthesis_of_major_deposit_types

[2] G. M. Mudd and S. M. Jowitt, "Growing global copper resources, reserves and production: Discovery is not the only control on supply," *Econ. Geol.*, vol. 113, no. 6, pp. 1235–1267, Sep. 2018, doi: 10.5382/ECONGEO.2018.4590.

[3] M. I. A. Shakirullah, "Mineral development profile of North West Frontier Province and the role of Directorate General Mines and Minerals in the mineral resources development," Journal of Himalayan Earth Sciences. Accessed: Feb. 24, 2025. [Online]. Available: http://ojs.uop.edu.pk/jhes/article/view/1581

[4] L. A. Naveed Anjum, M. Arif, "Mineralogical and beneficiation studies of the fe-cu ores of dammal nisar, chitral, NW himalayas Pakistan," Journal of Himalayan Earth Sciences. Accessed: Feb. 24, 2025. [Online]. Available: https://www.researchgate.net/publication/330839415_Mineralogical_and_beneficiation_studies_of_the_fe-cu_ores_of_dammal_nisar_chitral_NW_himalayas_Pakistan

[5] Richard H Sillitoe, "Supergene oxidized and enriched porphyry copper and related deposits," Google Search. Accessed: Feb. 24, 2025. [Online]. Available: https://www.google.com/search?q=Supergene+oxidized+and+enriched+porphyry+copper+and+related+deposits&rlz=1C1BNSD_enPK1109PK1109&oq=Supergene+oxidized+and+enriched+porphyry+copper+and+related+deposits&gs_lcrp=EgZjaHJvbWUyBggAEEUYOdIBBzYzMmowajeoAgCwAgA&sourceid=chrome&ie=UTF-8

[6] S. M. Bignold, P. J. Treloar, and N. Petford, "Changing sources of magma generation beneath intra-oceanic island arcs: An insight from the juvenile Kohistan island arc, Pakistan Himalaya," *Chem. Geol.*, vol. 233, no. 1–2, pp. 46–74, Sep. 2006, doi: 10.1016/J.CHEMGEO.2006.02.008.

[7] M. T. Shah and J. W. Shervais, "The Dir-Utror metavolcanic sequence, Kohistan arc terrane, northern Pakistan," *J. Asian Earth Sci.*, vol. 17, no. 4, pp. 459–475, Aug. 1999, doi: 10.1016/S1367-9120(99)00009-7.

[8] S. K. Shahbaz Alam, Ishfaq Ahmad, "Physio-Mechanical and Petrographic Characteristics of Granitic Rocks from the Demote Valley, Gilgit, Pakistan: Implications for Strength and

Bearing Capacity," International Journal of Innovations in Science & Technology. Accessed: Feb. 24, 2025. [Online]. Available: https://www.researchgate.net/publication/387998091_Physio-Mechanical_and_Petrographic_Characteristics_of_Granitic_Rocks_from_the_Demote_Valley_Gilgit_Pakistan_Implications_for_Strength_and_Bearing_Capacity

[9] W. R. A. B. T. N. Irvine, "A Guide to the Chemical Classification of the Common Volcanic Rocks |," Canadian Journal of Earth Sciences. Accessed: Feb. 24, 2025. [Online]. Available: https://pubs.geoscienceworld.org/csp/cjes/article/8/5/523/55081/A-Guide-to-the-Chemical-Classification-of-the

[10] M. J. L. Bas, R. W. L. Maitre, A. Streckeisen, and B. Zanettin, "A Chemical Classification of Volcanic Rocks Based on the Total Alkali-Silica Diagram," *J. Petrol.*, vol. 27, no. 3, pp. 745–750, Jun. 1986, doi: 10.1093/PETROLOGY/27.3.745.

[11] Z. Cheng *et al.*, "Geochemistry and petrogenesis of the post-collisional high-K calc-alkaline magmatic rocks in Tengchong, SE Tibet," *J. Asian Earth Sci.*, vol. 193, p. 104309, May 2020, doi: 10.1016/J.JSEAES.2020.104309.

[12] E. D. Mullen, "MnO/TiO2/P2O5: a minor element discriminant for basaltic rocks of oceanic environments and its implications for petrogenesis," *Earth Planet. Sci. Lett.*, vol. 62, no. 1, pp. 53–62, Jan. 1983, doi: 10.1016/0012-821X(83)90070-5.

[13] J. D. Tony Barresi, "Geochemistry and Petrography of Upper Hazelton Group Volcanics: VHMS- Favourable Stratigraphy in the Iskut River and Telegraph Creek Map Areas," Northwestern British Columbia. Accessed: Feb. 24, 2025. [Online]. Available:

[14] A. Miyashiro, "Volcanic Rock Series in Island Arcs and Active Continental Margins," *Am. J. Sci.*, vol. 274, no. 4, pp. 321–355, 1974, doi: https://doi.org/10.2475/ajs.274.4.321.

[15] R. A. Batchelor and P. Bowden, "Petrogenetic interpretation of granitoid rock series using multicationic parameters," *Chem. Geol.*, vol. 48, no. 1–4, pp. 43–55, Mar. 1985, doi: 10.1016/0009-2541(85)90034-8.

[16] V. B. Khubanov, A. A. Tsygankov, and G. N. Burmakina, "The duration and geodynamics of formation of the angara–vitim batholith: Results of u–pb isotope (la-icp-ms) dating of magmatic and detrital zircons," *Russ. Geol. Geophys.*, vol. 62, no. 12, pp. 1331–1349, Dec. 2021, doi: 10.2113/RGG20204223.

[17] K. M. H. Leon Gläser, Anna Grosche, Panagiotis C. Voudouris, "The high-K calc-alkaline to shoshonitic volcanism of Limnos, Greece: implications for the geodynamic evolution of the northern Aegean," *Contrib. to Mineral. Petrol.*, vol. 177, no. 73, 2022, doi: https://doi.org/10.1007/s00410-022-01940-7.

[18] M. Abu-Fatima, C. Marignac, M. Cathelineau, and M. C. Boiron, "Metallogeny of a Pan-African oceanic arc: VHMS and gold deposits in the Ariab-Arbaat belt, Haya terrane, Red Sea Hills (Sudan)," *Gondwana Res.*, vol. 98, pp. 76–106, Oct. 2021, doi: 10.1016/J.GR.2021.06.001.

[19] M. P. R. Irene del Real, Martin Reich, Adam C. Simon, Artur Deditius, Fernando Barra, María A. Rodríguez-Mustafa, John F. H. Thompson, "Formation of giant iron oxide-copper-gold deposits by superimposed, episodic hydrothermal pulses," *Commun. Earth Environ.*, vol. 2, no. 1, p. 192, 2021, doi: 10.1038/s43247-021-00265-w.

[20] L. Mathieu, "Quantifying Hydrothermal Alteration: A Review of Methods," *Géosciences*, 2018, doi: 10.3390/GEOSCIENCES8070245.

[21] Anne M. Sasso, "GEOLOGICAL EVOLUTION AND METALLOGENETIC RELATIONSHIPS OF THE FARALLON NEGRO VOLCANIC COMPLEX, NW ARGENTRVA," *Qrreen's Univ. Kingsron, Ontario, Canad*, 1997, [Online]. Available: https://www.collectionscanada.gc.ca/obj/s4/f2/dsk3/ftp04/nq22508.pdf